**Analysis of acyl fluxes through multiple pathways of triacylglycerol synthesis in developing soybean embryos**

Philip D. Bates, Timothy P. Durrett, John B. Ohlrogge, and Mike Pollard

## SUPPLEMENT

### Supplement: Kinetic Modeling of Pool Filling

The goal of the following analysis is to choose between alternative models of TAG synthesis which take into account various options for DAG-PC interconversions. Simulations of pool filling for various models (Figures S8 and S9) were undertaken to determine how each model would match the observed kinetic labeling data. The expectation was not that any of the more complex models would exactly match the actual kinetics measured (Figures 2, 7). Instead the modeling is used to formulate the best descriptions of acyl metabolism.

In such modeling of the *in vivo* data there is a list of implicit assumptions:
(1) The cells are in a relatively uniform physiological state. At this stage of soybean embryo development cell differentiation and division have essentially ceased. The embryo has entered the maturation phase and all cells are expected to be accumulating storage products. Some small differences in development and gene expression of cells can be expected across the tissues. Thus we model an average value.
(2) Although exogenous “non-physiological” substrates may penetrate differently and may perturb metabolism slightly differently, they effectively report the bulk tissue metabolism. This was the case for our leaf labeling experiments (Bates et al., 2007)
(3) *In vivo* variance, including that generated by using different experiments used for acetate and glycerol labeling is small. This assumption is supported by replicate experiments.

(4) We assume that there is negligible futile cycling of acyl groups through FA synthesis and β-oxidation, that TAG is a static end product within the short time frame of the experiments, and that different lipid molecular species of a lipid class have similar time constants for pool filling.
(5) Minor acyl fluxes, such as to sphingolipids, plastid lipids, PE etc. which are not specifically modeled have only a minor influence on the major quantitative conclusions.

The modeling is set up with 1000 moles FA in total PC and 400 moles in total DAG (from Table 1), which are invariant in size over the period of one hour for which the simulation is run. The inputs are either 100 moles/hr of FA into the system through the DAG(*de novo*) pool, or 300 moles via acyl editing into a bulk or small active PC pool. The output is 100 moles/hr of FA into TAG. The 300 moles for acyl editing is chosen based on an approximately average value between maximum and minimum values that can be inferred (see next section or Figure 10). A simple Excel spreadsheet (available from the corresponding author) is used to run the simulation, using 0.01 hour increments, that is, with 1 mole FA input per time increment when modeling for *de novo* DAG input. The models simulated are based off those represented in Figure S8. In the case of the simplest model tested, model B (Figure S9a) (Griffiths et al., 1988), the rate constant for DAG to TAG conversion $k_1$ will be 0.25 $hr^{-1}$, to allow a fixed rate of TAG synthesis of 100 moles/hr (400 moles DAG x 0.25 $hr^{-1}$). The rate constants for the DAG to PC ($k_2$) and PC to DAG conversions ($k_3$) can be set at any value, but because the DAG and PC pool sizes must be kept constant, the ratio of $k_2$:$k_3$ = 2.5. The values of $k_2$ and $k_3$ were then varied to allow a simulation of glycerol backbone labeling from DAG that produced continuous DAG labeling but where PC labeling crossed over DAG labeling at about 30 minutes as in the experimental results (Figure 7A). This occurred when the forward and back reactions for the DAG to PC interconversion were 20 times the rate of TAG synthesis (Figure S9a). These parameters were then used to test the prediction for an acyl editing input (Figure S9b). Acyl editing simulations have included a

loop to allow some of the edited acyl groups to be used for *de novo* DAG synthesis. At 30 minutes about 21% of the PC would be converted to DAG. This is inconsistent with experimental observations that show about 3% of the PC have actually moved from PC to DAG. Thus model B fails to predict the slow movement of labeled PC to DAG. If at 0.5 hr 21% PC was converted to DAG that would change the composition and stereochemistry of the DAG product dramatically.

Additional pool filling simulations for Models B and C (including variants) were run to see how closely they would conform to the experimental kinetics of glycerol backbone labeling, of TAG labeling, and of acyl editing. Some of these are shown in Figure S9. Variants on model B suffered the same problem as the simplest form of model B (too much back conversion of acyl labeled PC to DAG at early time points). By contrast, variants on model C were generally much more successful at describing the DAG-PC precursor-product glycerol labeling kinetics and yet having slow movement of the acyl editing labeling of PC move through into DAG. Model C variants have as a common theme at least two kinetically distinct DAG pools, the input pool DAG(*de novo*) for the immediate products of *de novo* DAG synthesis, and the output pool DAG(oil synth), which supplies TAG synthesis. The DAG input pool is kept small (2% of PC), in keeping with the observation of very small DAG pools associated with PC synthesis in leaf, constituting less than 1% of total PC (Mhaske and Pollard, unpublished observations); because the *de novo* DAG pool must be compositionally distinct from the bulk DAG pool; and because glycerol labeled DAG moves through to PC very significantly within 30 minutes (PC pool filling to TAG takes 10 hours, so if 15 min pool filling of DAG occurs, it will be 1/40 of PC). The fit for the most simplified version of Model C ($\rightarrow$ DAG $\rightarrow$ PC $\rightarrow$ DAG $\rightarrow$TAG) gives a rather flattened DAG filling curve (Figure S9c) compared to the experimental data in Figure 7a, although this can be attenuated by adding a direct low flux loop from DAG(*de novo*) to DAG(oil synth). Thus Model C, variant 1 seems unlikely.

Splitting the PC pool into a small, active pool and a large, bulk pool as shown in Model C, variant 2 (Figures S8 and S9d) greatly alleviates the problem of slow DAG pool filling at later times seen in Model C, variant 1. Keeping the active PC pool at 2% of the total PC, and therefore at the same size as DAG(*de novo*), requires that the interchange between the active and bulk PC pools be 3 times the rate of TAG synthesis. If this is done, then acyl editing must be largely a function of the bulk pool (Figure S9e), not the active pool (Figure S9f). In proposing two PC pools, it is not clear whether the desaturases act on PC during its residence in the small, active PC pool, or the bulk PC pool, or both. Longer term labeling studies are required to resolve this issue. One problem with simulations of Model C, variants 1 (Figure S9c) and 2 (Figure S9d), was that they predicted movement of glycerol labeling into TAG that was much slower than observed (Figure 7A). This could be remedied by splitting the DAG(oil synth) pool into a small active and a large bulk component (Figure S8 Model C, variant 3 and Figure S9g). Splitting the DAG pools in this way has minimal effect on the acyl editing simulations shown in Figures S9e and S8f. Of course, with multiple TAG synthesis routes, this partitioning of DAG(oil synth) may still be a simplification. More generally, the splitting of the intermediate pools of PC and DAG allows for a large degree of flexibility in modeling TAG synthesis, with many combinations of pool sizes and exchange rates. The exercise of modeling initial kinetics has lead to Model C, variant 3 as our preferred model, giving a reasonable though not an exact simulation. However, many more complex variants are possible and cannot be adequately distinguished. Clearly, additional methods, such as longer term and pulse-chase labeling, will be required to refine the model.

## Supplement: Discussion of Soybean TAG Synthesis Flux Model Shown in Figure 10

In addition to the assumptions described at the beginning of the previous section the following features are used to generate a model of acyl group fluxes in soybean embryos. These features are derived from the endogenous lipid

compositions and from the [$^{14}$C]acetate and [$^{14}$C]glycerol labeling results and conclusions presented in the Results and Discussion sections.

1) *De novo* synthesis of DAG and acyl editing of PC are metabolically distinct processes.

2) Nascent FAs are directly incorporated into PC through *sn*-1 and *sn*-2 acyl editing.

3) Nascent FAs can mix with recycled FA released from acyl editing for *de novo* glycerolipid synthesis.

4) The major flux of *de novo* synthesized DAG is for PC synthesis.

5) TAG synthesis is associated with the bulk DAG pool generated from bulk PC, and not with *de novo* synthesized DAG.

6) The bulk DAG generating reaction is in a different location such that *de novo* synthesized PC and acyl edited PC are not rapidly used for TAG synthesis.

7) In a soybean embryo rapidly accumulating oil 93% of FAs are ultimately used for TAG synthesis and most of the PC/DAG produced is turned over for TAG synthesis.

8) Newly synthesized FAs are incorporated into PC, DAG and the sn-3 position of TAG at relative initial rates of approximately 10:3:2, respectively. Thus the initial FAS product incorporation into glycerolipids: 57% PC, 17% DAG, 11% TAG (total 85%).

Step by step logic in flux model construction

The model (Figure 10) tracks acyl fluxes over a very short time increment during which 100 moles of FAs are synthesized by the plastid. During this time increment these nascent FAs are exported from the plastid and undergo their initial incorporations into glycerolipids. Model construction utilizes mass balance along with the initial FA incorporation rates and compositions. Newly synthesized FA are incorporated into PC, DAG and TAG at relative initial rates of 10:3:2, respectively. Thus the initial FAS product incorporation into glycerolipids: 57% PC, 17% DAG, 11% TAG, with the remaining 15% distributed among other

products (Table S3). If 93 moles of FA are ultimately incorporated into TAG (based on Table 1, and the fact that PC represents ~1/2 of soybean membrane lipids) and the remaining 7 moles provide for membrane lipid synthesis then 31 and 3.5 moles of G3P are required for acyl group esterification, respectively. *De novo* synthesis of 34.5 moles of total glycerolipids would require 69 moles of FAs to flux through PA and DAG into the *sn*-1/*sn*-2 positions of membrane lipids and TAG. The remaining 31 moles of FAs will be esterified to the *sn*-3 position of TAG. If between 17 and 32 moles of nascent [$^{14}$C]FA are used by *de novo* glycerolipid synthesis (Table S3, DAG and DAG + other), then an additional 62 to 37 moles of recycled [$^{12}$C]FA are required to balance *de novo* synthesis. Presumably this is provided by the acyl chains released by acyl editing to allow 57 moles of nascent [$^{14}$C]FAs to be incorporated into PC through lyso-PC acylation. However, 57 mol of PC acyl editing will not provide enough saturates to sustain *de novo* glycerolipid synthesis. Saturates make up ~29% of acyl groups entering *de novo* glycerolipid synthesis, as estimated from [$^{14}$C]glycerol labeling (Figure S7). Thus total saturates would comprise 20 moles of the 69 moles acylated to G3P. Newly synthesized FA would contribute 4.9 to 9.3 moles of saturates (Table S3), requiring 15.1 to 10.7 moles of recycled saturates. However, 57 mol of PC acyl editing observed through nascent FA incorporation into PC was 14% *sn*-1 and 86% *sn*-2. Saturates are predominately at the *sn*-1 position, therefore if the labeling reflects the positional release of FA during acyl editing much less saturates would be released and recycled into *de novo* synthesis. More quantitatively, if acyl editing is only represented by the release of 57 moles of [$^{12}$C]FA, and *sn*-1 acyl editing is completely saturated FA specific, 8 moles of [$^{12}$C]S can be provided. However, if sn-1 acyl editing is relatively non-specific, this drops to about 3.7 moles of [$^{12}$C]S. Therefore the flux of acyl editing cannot be one acyl group released from PC for each nascent acyl group incorporated, and must be at least 1.4 times that required for incorporation of nascent FA into PC with the possibility of being very much greater, up to 4.1 times based on the above argument. The excess flux of recycled acyl groups produced during acyl editing may be re-incorporated into PC through the acyl

editing cycle (Figure 10), with the entire process reducing the saturated concentration of PC and redistributing FA between the *sn*-1/*sn*-2 positions.

Initially labeled PC and DAG show different [$^{14}$C]FA incorporation rates and compositions. This could indicate that there are different acyl-CoA pools with distinctly different proportions of new and recycled acyl groups feeding *de novo* glycerolipid synthesis and PC acyl editing, or that the acyl editing flux is selective and fast enough that over three times as much nascent FA from the same mixed pool enter PC through acyl editing rather than enter DAG (Figure 2). Although nascent acyl groups could be channeled directly into lyso-PC that is under a high flux of reacylation with recycled acyl groups, we consider it more likely that nascent acyl groups mix with the recycled acyl groups of the rapid acyl editing cycle. We have shown this simpler alternative in Figure 10. To estimate the relative flux of acyl groups around the acyl editing cycle we consider how many more FA must be removed from the mixed acyl pool by acyl editing compared to *de novo* synthesis to produce the different [$^{14}$C]FA labeling amounts and stereochemistry of PC and DAG. To simplify the compositional and stereochemical differences of acylation we consider the relative flux of [$^{14}$C]M into the *sn*-2 position of both lipids, using initial labeling values for PC to be 100% *sn*-2 M and for DAG to be 50% *sn*-2 M. In this scenario 54.1 moles nascent [$^{14}$C]M enter *sn*-2 PC while 6.05 to 11.35 moles enter *de novo* glycerolipid synthesis (Table S3, DAG to DAG + other). Therefore the flux of nascent [$^{14}$C]M into the *sn*-2 position of PC is a maximum of 8.9 to 4.8 times faster than esterification into the *sn*-2 position of DAG (via PA). This comparison assumes that the utilization of labeled oleate in the mixed acyl-CoA pool reports the relative flux of the two reactions, and therefore assumes negligible discrimination between M, D and T for *sn*-2 acylation and exchange. However, if there is any enzymatic selectivity for LPAT or acyl editing enzymes the flux ratios could change. There is no enzymology data available for soybean. The additional unlabeled saturates required for *de novo* DAG synthesis can be explained by either accepting the acetate labeling as reporting the correct ratio for *sn*-1 versus *sn*-2 acyl editing (Figure 4), and postulating that the acyl editing turnover is much more rapid than

that observed directly, or by postulating that there is a “hidden” *sn*-1 acyl editing component due to recycling of non-labeled saturates and other acyl groups. Certainly, in pea leaf, the PC *sn*-1 acyl editing activity is much closer to that exhibited by *sn*-2 acyl editing (Bates et al., 2007). In the former case, a ratio of 8.9:1 for *sn*-2 fluxes for PC editing versus DAG synthesis translates to 5.1 for total (*sn*-1 plus *sn*-2) fluxes. If the PC *sn*-1 acyl editing flux equals the *sn*-2 acyl editing flux, then the ratio remains the same.

TAG synthesis will require 31 moles of *sn*-3 acylation. About 11 moles of this flux is provided by the immediate incorporation of nascent FA, with a high preference for saturates (Table S3). Analysis of the molecular species of [$^{14}$C]FA labeled TAG suggests that this direct acylation utilizes the bulk DAG pool, not the *de novo* synthesized DAG pool, and provides about 35% of the molecular species in endogenous TAG. The other 65% of TAG synthesis would be compensated by utilizing the recycled acyl-CoA pool from acyl editing and also PDAT reactions.

**Supplemental Method and Discussion for Figure S2 – Chemical alpha-Oxidation:** The totaled labeled saturated FA accumulation from [$^{14}$C]acetate labeling produced 18:0>16:0 (Figure S1). This distribution was also noted in the individual lipid classes, and is an inversion of the endogenous composition, where 16:0>18:0. The reason for this inversion in labeling is not known. Chemical $\alpha$-oxidation demonstrated that the [$^{14}$C]label was evenly distributed along the [$^{14}$C]18:0 acyl chain (Supplement Figure S2). This result suggested that the 18:0 was a direct product of fatty acid synthesis and not labeled by a high specific activity cytosolic elongation as reported for other very long chain FA (Pollard and Stumpf, 1980a, 1980b).

To conduct the analysis of the position of the label, individual saturated FAME from TAG and PC were collected by first $AgNO_3$ then reversed phase TLC (as in methods) and saponified to give the individual free fatty acids. Unlabeled carrier FA (0.1 mg) was added to each reaction with the respective FA chain length. The reaction was started by adding 10 mg of finely ground $KMnO_4$ and

0.5 ml acetone to each dried FA sample and heated to 60° C for six hours. On cooling the remaining $KMnO_4$ was reduced by adding 1 ml of 0.5M $FeSO_4$ in 0.5 N $H_2SO_4$. FA were extracted with hexane and FAME generated by methylation in 5% sulfuric acid in MeOH at 50° C for 30 min. FAME extracted by hexane were split into two aliquots, mass quantified by GC-FID, and radioactivity quantified by reversed phase TLC and electronic autoradiography.

**Pollard MR, Stumpf PK** (1980) Biosynthesis of C-20 and C-22 fatty-acids by developing seeds of Limnanthes-alba - chain elongation and delta-5 desaturation. Plant Physiol **66:** 649-655

**Pollard MR, Stumpf PK** (1980) Long-chain (C-20 and C-22) fatty-acid biosynthesis in developing seeds of Tropaeolum-majus - an in vivo study. Plant Physiol **66:** 641-648

## Supplemental Method for Tables S1 and S2 - Endogenous Molecular Species Compositions

Total lipids from four soybean embryos (13-14 mg dry weight), cultured under identical conditions to those used for labeling, were extracted according to Hara and Radin (1978). TAG concentrations were measured directly using electrospray ionization mass-spectrometry (ESI-MS). DAG and PC were converted to their *sn*-1,2-diacyl-3-acetyl-glycerol (ac-TAG) derivatives by digestion with pancreatic lipase C (for PC) followed by acetylation prior to ESI-MS analysis. ESI-MS in positive ion mode was performed by direct infusion with a Shimadzu (Columbia, MD) SIL-5000 autosampler into a Waters (Milford, MA) Quattro micro mass spectrometer. 10µl of sample in toluene was introduced to the electrospray source by flow injection analysis conveyed by a 65:32:3 chloroform:methanol:100mM ammonium acetate solution at a flow rate of 0.1 ml/min. The capillary, extractor, and cone voltages were 3.2 kV, 2.0 V, and 40 V respectively. The source and desolvation temperatures were 110 and 350 °C,

respectively. The desolvation gas flow rate was 400 l/hr. Mass spectra were collected for 2 min; the *m*/*z* range scanned in the MS measurements was from 500 to 1000 (1 sec/scan) and in the $MS^2$ measurements from 20 to the mass of the parent ion. Collision-induced dissociation used argon as the collision gas ($2 \times 10^{-3}$ mbar) with the collision energy set at 22 eV. Mass spectra data was acquired with MassLynx 4.0 software; $[TAG\text{-}NH_4]^+$ ion peaks were smoothed and integrated using QuanLynx software.

In order to correct for the effect of the number of acyl chain carbons and double bonds on the signal strength (Han and Gross, 2001), TAG standards with varying acyl chain length and number of double bonds were analyzed at different concentrations. After correcting for natural isotope abundance effects, the ion peak intensities for each TAG standard were normalized to the internal standard (10µM triheptadecanoin). The normalized peak intensity was plotted against TAG concentration. The slope of this standard curve was determined for each TAG standard. Multiple linear regression was then used to create a correction function relating the slope of the standard curve to the number of acyl chain carbons and double bonds.

To determine the concentration of soybean TAG or acetylated-DAG molecular species, the ion peak intensities were corrected for overlap from the natural isotope abundance clusters of other peaks and then normalized to the 10µM triheptadecanoin internal standard. The correction function for acyl chain carbons and double bonds was then applied to determine the absolute concentration of each TAG species. When necessary, ESI-$MS^2$ was used to determine the relative abundance of isomers with the same *m*/*z* value. The moles $embryo^{-1}$ of each molecular species measured for TAG, DAG, PC are provided in supplemental tables SI, SII, SIII, respectively.

## Supplement Tables

### Table 1

| TAG Molecular Species | nmoles TAG/embryo |
|---|---|
| PPI | 4.19 ± 0.17 |
| PPL | 12.92 ± 0.35 |
| PPO | 4.52 ± 0.35 |
| PPS | 0.66 ± 0.27 |
| PLL | 8.03 ± 0.28 |
| PLI | 26.86 ± 1.23 |
| PLL | 38.60 ± 1.11 |
| POI | 15.78 ± 0.45 |
| POL | 37.72 ± 2.13 |
| PSI | 2.16 ± 0.12 |
| POO | 13.70 ± 0.26 |
| PLI | 9.26 ± 0.18 |
| PSO | 6.02 ± 0.78 |
| LII | 14.10 ± 0.77 |
| LLI | 34.12 ± 1.82 |
| OII | 7.40 ± 0.39 |
| OLT | 39.06 ± 1.75 |
| LLL | 28.94 ± 1.29 |
| SII | 1.33 ± 0.05 |
| OLL | 43.15 ± 1.75 |
| OOI | 12.88 ± 0.52 |
| SLI | 7.69 ± 0.31 |
| OOL | 28.44 ± 2.06 |
| OLL | 10.49 ± 0.76 |
| SOI | 5.27 ± 0.38 |
| SOL | 16.20 ± 0.76 |
| OOO | 11.95 ± 0.56 |
| SSI | 0.79 ± 0.03 |
| SOO | 8.23 ± 0.40 |
| SSL | 2.97 ± 0.14 |
| SSO | 3.35 ± 0.21 |
| ALL | 2.43 ± 0.09 |
| AOI | 2.85 ± 0.11 |
| AOL | 3.70 ± 0.20 |

**Table S1:** TAG molecular species composition in developing soybean embryos. Individual TAG molecular species of developing soybean embryos were quantified using ESI-MS and ESI-MS$^2$. Values represent nanomoles of TAG per embryo (± standard deviation). Descriptions of the various molecular species do not imply any specific stereochemical arrangement of the different acyl chains. Abbreviations for fatty acids: P = palmitate (16:0), S = stearate (18:0), O = oleate (18:1), L = linoleate (18:2), I = linolenate (18:3) and A = arachidonate (20:0).

**Table 2**

| Molecular Species | pmoles DAG/embryo | pmoles PC/embryo |
|---|---|---|
| PP | 20 ± 3 | 952 ± 119 |
| PLn | 385 ± 23 | 832 ± 97 |
| PL | 1630 ± 146 | 3827 ± 456 |
| PO | 878 ± 81 | 2142 ± 245 |
| PS | 81 ± 12 | 524 ± 76 |
| LnLn | 126 ± 10 | 524 ± 98 |
| LLn | 751 ± 40 | 1837 ± 218 |
| OLn | 537 ± 30 | 1244 ± 129 |
| LL | 1364 ± 76 | 3484 ± 361 |
| SLn | 131 ± 8 | 359 ± 38 |
| OL | 1884 ± 120 | 4360 ± 460 |
| SL | 693 ± 44 | 1913 ± 187 |
| OO | 1240 ± 79 | 2964 ± 289 |
| SO | 594 ± 47 | 1731 ± 166 |
| SS | 106 ± 11 | 259 ± 44 |

**Table S2:** DAG and PC molecular species compositions in developing soybean embryos. DAG and PC molecular species of developing soybean embryos were converted to their *sn*-1,2-diacyly-3-acetyl-glycerol derivatives and then quantified using ESI-MS and ESI-MS$^2$. Values represent picomoles of DAG per embryo (± standard deviation). Descriptions of the various molecular species do not imply any specific stereochemical arrangement of the different acyl chains. Abbreviations for fatty acids: P = palmitate (16:0), S = stearate (18:0), O = oleate (18:1), L = linoleate (18:2), and Ln = linolenate (18:3).

**Table 3**

| Lipid Classes | Distribution of [$^{14}$C]Acyl Groups | | | Acyl fluxes | |
|---|---|---|---|---|---|
| | Within Total Lipids (%) | Within Each Lipid Class | | | |
| | | S (% $^{14}$C) | M (% $^{4}$C) | Nascent S | Nascent M |
| **PC** | 57 | 5 | 95 | 2.9 | 54.1 |
| **DAG** | 17 | 29 | 71 | 4.9 | 12.1 |
| **TAG** | 11 | 75 | 25 | 8.2 | 2.8 |
| **Other** | 15 | 29 | 71 | 4.4 | 10.6 |
| **DAG + Other** | 32 | | | 9.3 | 22.7 |

**Table S3:** TAG synthesis modeling - nascent FA flux value calculations. The percentage distribution of [$^{14}$C]acetate-labeled acyl groups between lipid classes is combined with the distribution of newly synthesized saturated (S, 16:0, 18:0) and monounsaturated (M, 18:1) FA in each lipid class to produce the nascent acyl flux (total = 100 moles per unit time and tissue). Total [$^{14}$C]FA values are based on the fact that 85% of newly synthesized FA are incorporated into PC, DAG and TAG, at a ratio of approximately 10:3:2, with the remaining 15% mainly incorporated into other membrane lipids.

## Supplement Figures

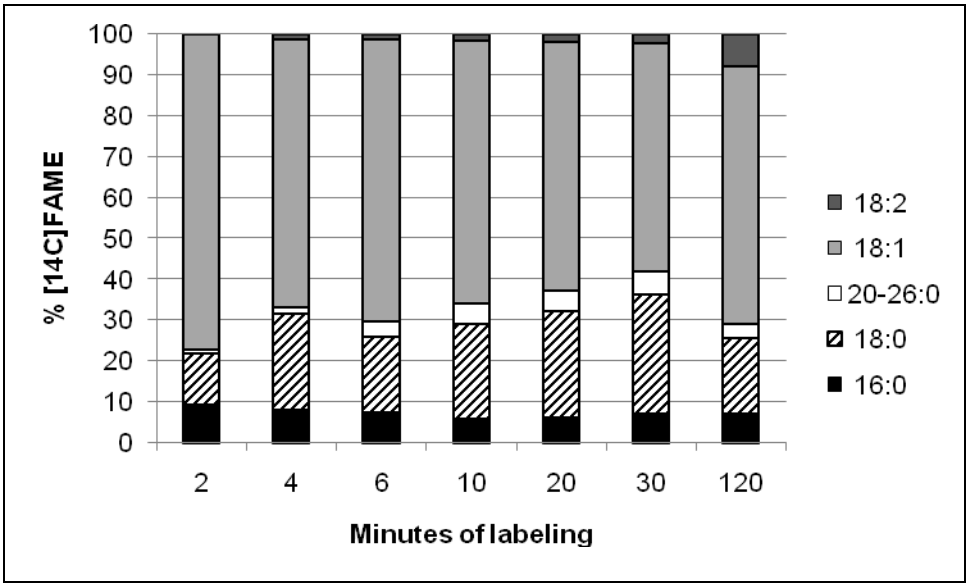


**Figure S1.** [$^{14}$C]Fatty acid composition of total lipids from labeling soybean embryos with [$^{14}$C]acetate for various times. FAMEs recovered from transmethylation of total lipids were separated based on the number of double bonds by $AgNO_3$-TLC and based on chain length/unsaturation by C18 reversed-phase TLC. Color labels: Black, 16:0; hatched, 18:0; white, the sum of 20:0, 22:0, 24:0, 26:0; light gray, 18:1; dark gray, 18:2.

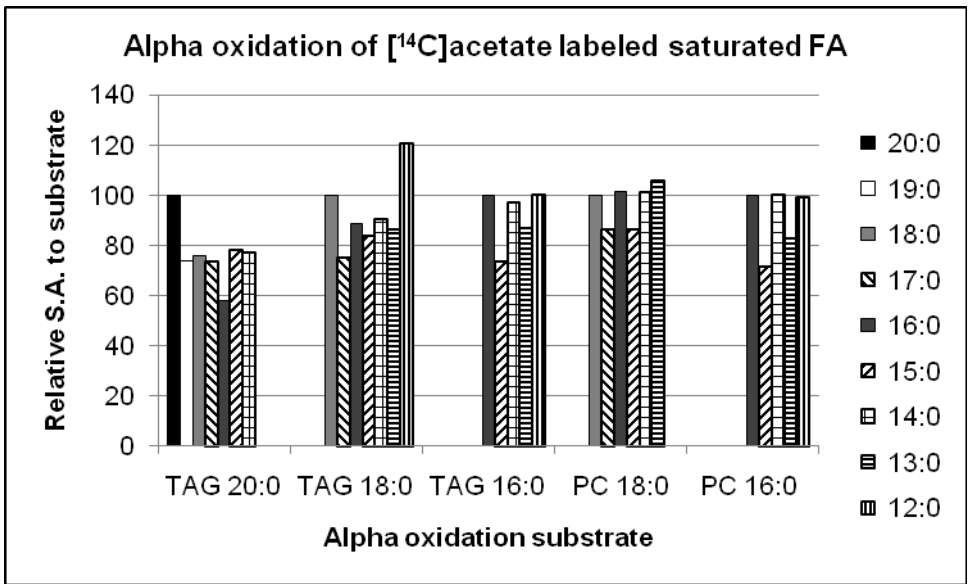


**Figure S2.** Alpha oxidation of [$^{14}$C]acetate labeled saturated FA from TAG and PC. Individual saturated FA acids from TAG and PC were subject to chemical alpha-oxidation. Each reaction is a mixture of FA from 20, 30, 120 & 360 min time points. The oxidation produced a series of FA each shortened by one carbon from the carboxyl end. Results are expressed as relative specific activity (S.A.) to that of the full length reaction substrate. The X-axis groups each individual substrate reaction products with decreasing chain length from left to right. Individual FA products bar shading is in the key.

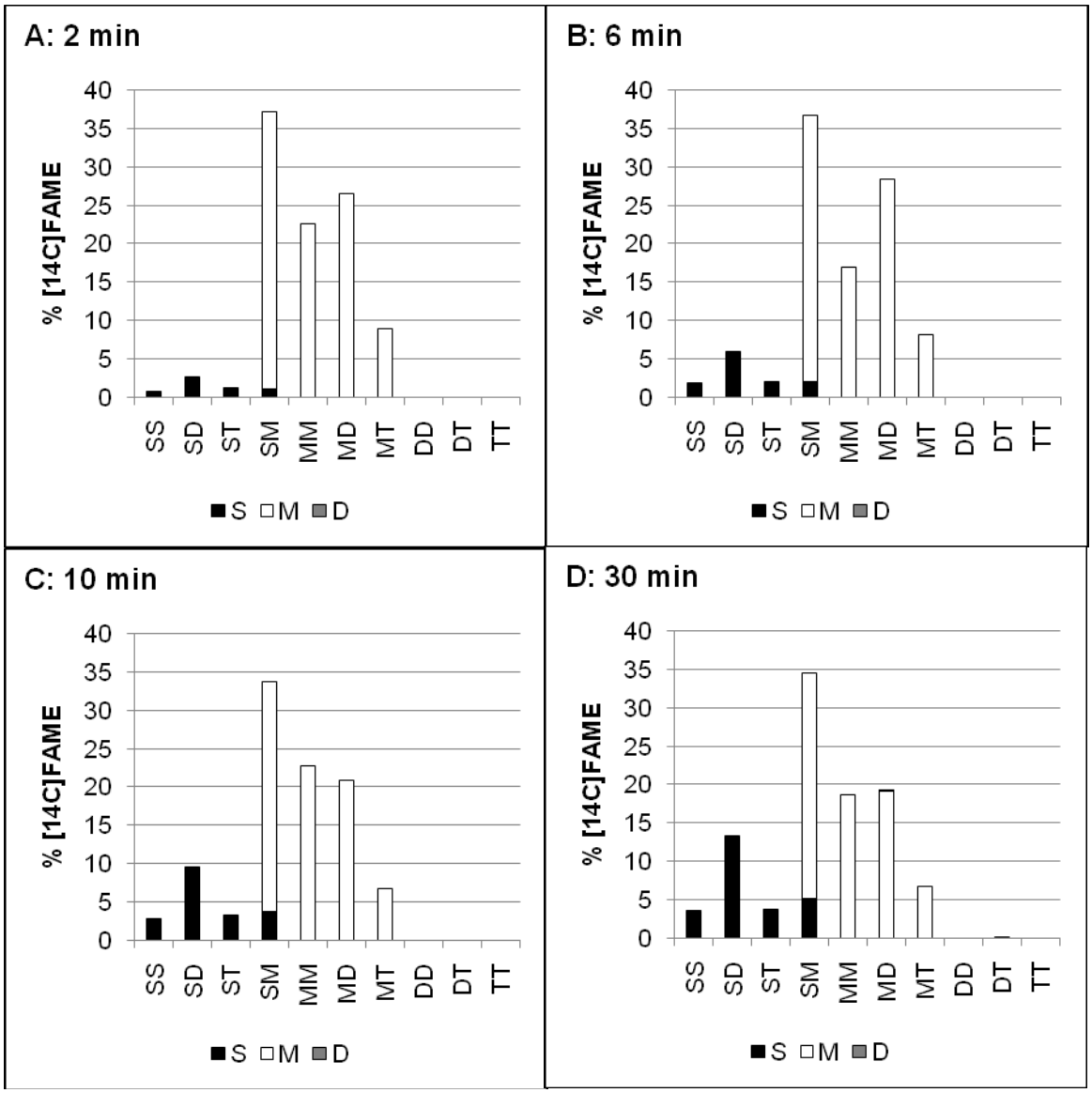


**Figure S3.** [$^{14}$C]Acetate labeled PC molecular species time course. A-D, molecular species are represented as pairs of FA, with bar heights represent % of species among the total labeled species. Bar shading represent % of [$^{14}$C]FA among species. In species with only one color it means that only that FA is labeled; the other FA within the molecular species is unlabeled. *Bar shading:* S, total saturates, black bars; M, monoenes (18:1), white bars; D, dienes (18:2), gray bars. A-D Time of [$^{14}$C]acetate labeling: A, 2 min; B, 6 min; C, 10 min; D, 30 min.

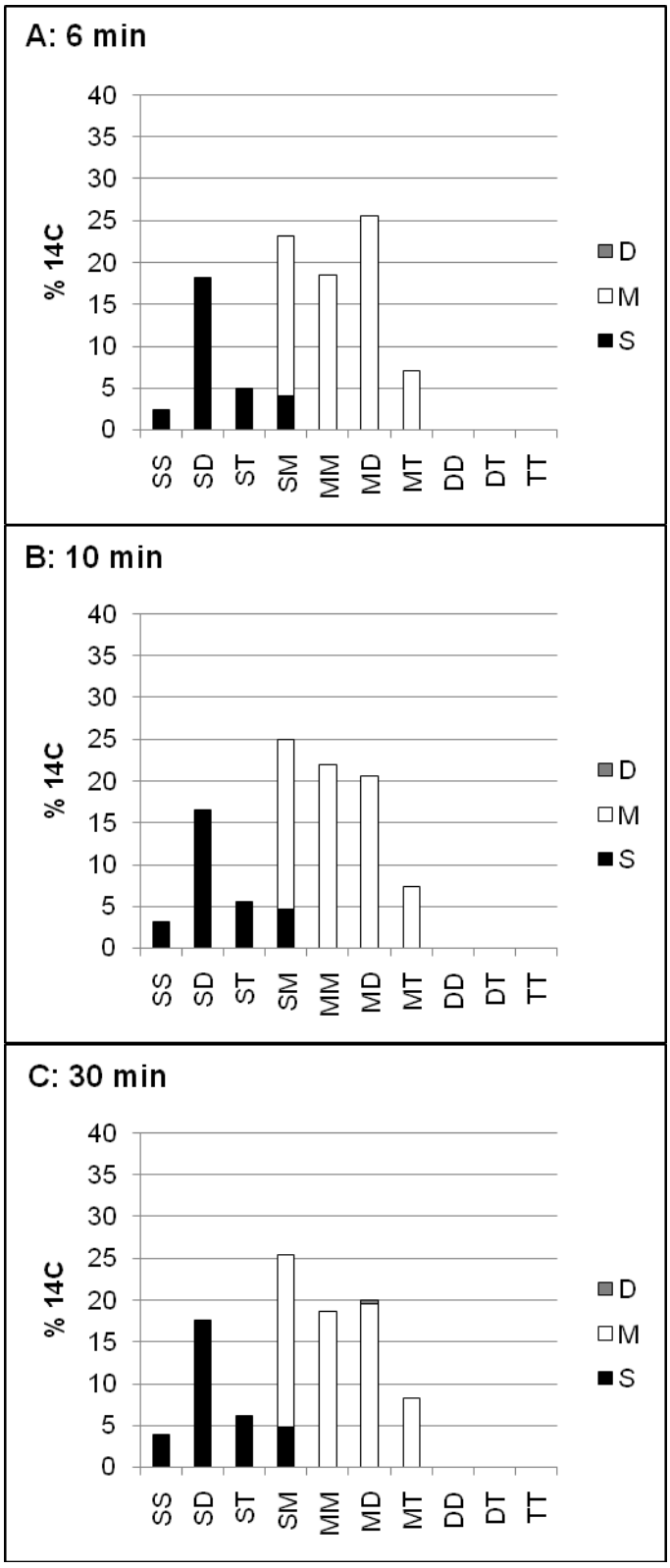


**Figure S4.** [$^{14}$C]Acetate labeled DAG molecular species time course. A-C, molecular species are represented as pairs of FA, with bar heights represent % of species among the total labeled species. Bar shading represent % of [$^{14}$C]FA among species. In species with only one color it means that only that FA is labeled; the other FA in the molecular species is unlabeled. *Bar shading:* S, total saturates, black bars; M, monoenes (18:1), white bars; D, dienes (18:2), gray bars. A-C, Time of [$^{14}$C]acetate labeling: A, 6 min; B, 10 min; C, 30 min.

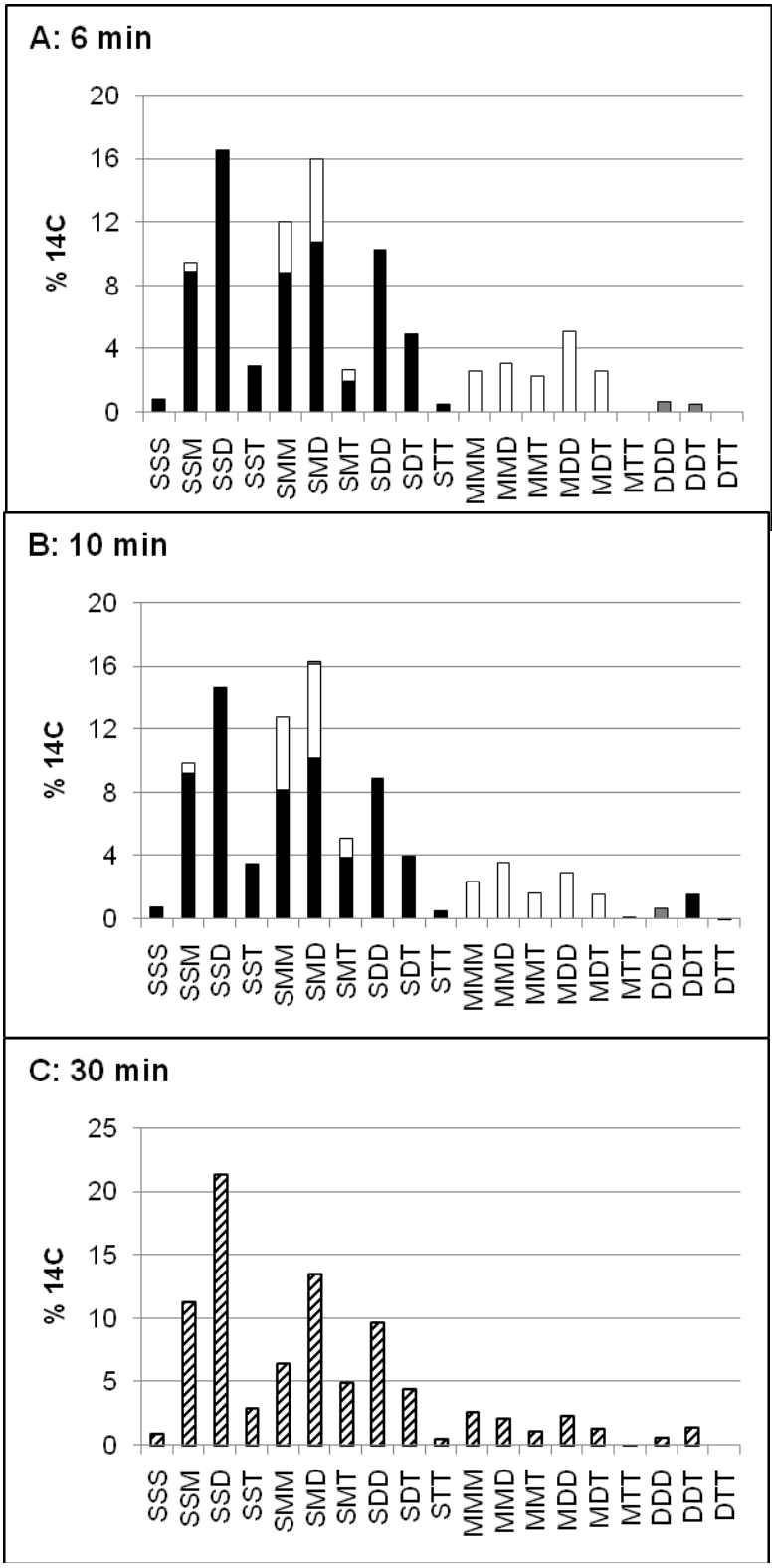


**Figure S5.** [$^{14}$C]Acetate labeled TAG molecular species time course. A-C, molecular species are represented as three of FA (no stereochemistry implied), with bar heights represent % of species among the total labeled species. A-B, bar shading represent % of [$^{14}$C]FA among species. In species with only one color it means that only that FA is labeled the other FA in the molecular species is unlabeled. *Bar shading:* S, total saturates, black bars; M, monoenes (18:1), white bars; D, dienes (18:2), gray bars. A, 6 min labeling; B, 10 min labeling; C, only the total [$^{14}$C]label per molecular species is reported.

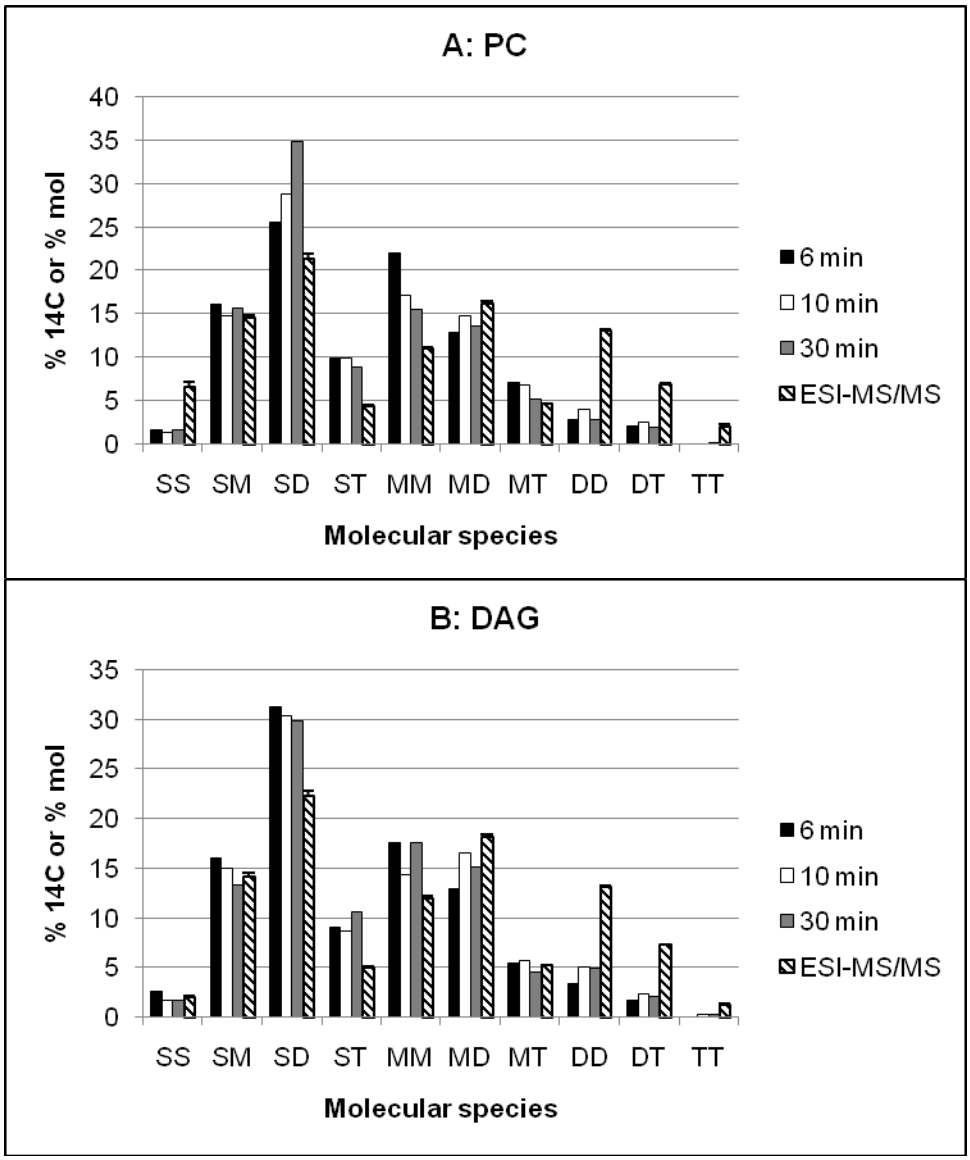


**Figure S6.** Time course of [$^{14}$C]glycerol labeled molecular species of PC (A) and DAG (B). A-B, molecular species are presented as a combination of two FA; total saturates, S; monoenes (18:1), M; dienes (18:2), D; trienes (18:3), T. [$^{14}$C]Glycerol labeled molecular species are backbone label only (acyl chain labeling has been subtracted). Bar shading represents labeling time: 6 min, black bars; 10 min, white bars; 30 min, gray bars. The endogenous mass molecular species compositions are ESI-MS/MS measurements from Figure 1, hatched bars.

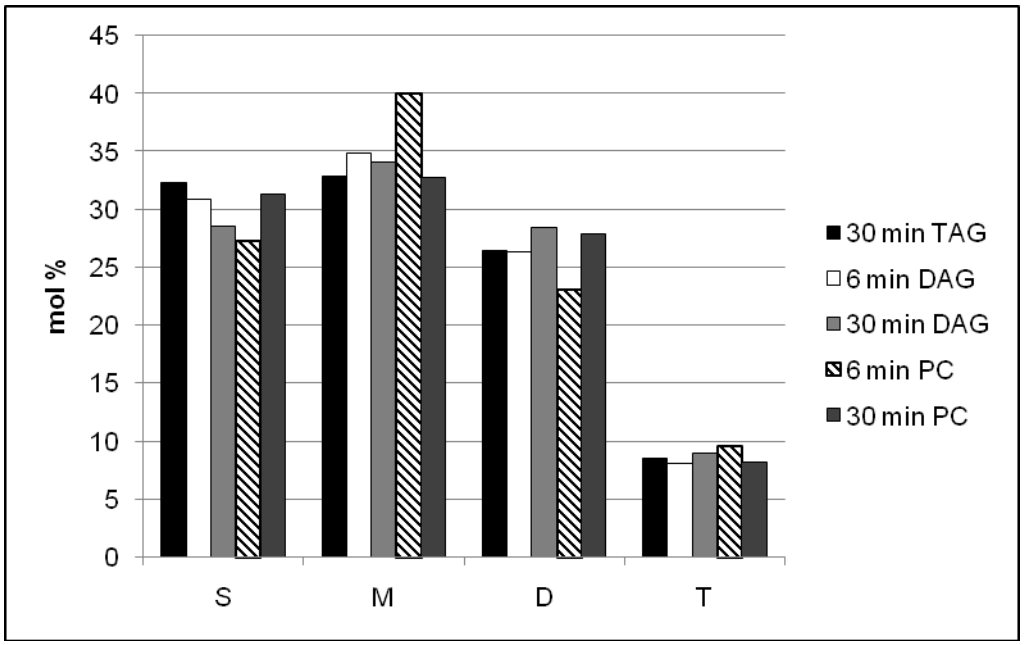


**Figure S7.** Fatty acid composition of [$^{14}$C]glycerol labeled TAG, DAG and PC molecular species. The composition represents the acyl groups esterified to glycerol-3-phosphate during *de novo* glycerolipid synthesis. Values are calculated from the [$^{14}$C]glycerol backbone labeled molecular species in Figures 8C (TAG) and S6 (PC and DAG). Fatty acids are: saturates, S; monoenes, M; dienes, D; trienes, T. Bar shading: 30 min TAG, black bars; 6 min DAG, white bars; 30 min DAG, light gray bars; 6 min PC, hatched bars; 30 min PC, dark gray bars.

**Model A**

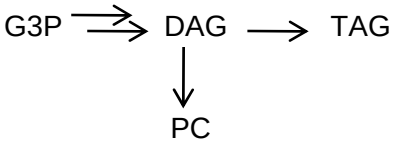


**Model B**

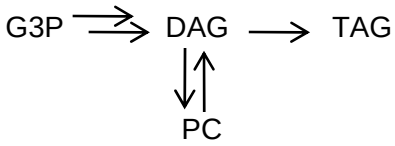


**Model B, variant 1**

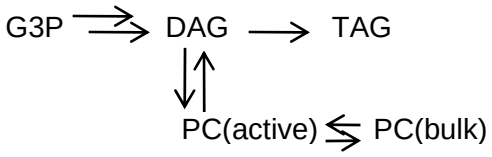


**Model C**

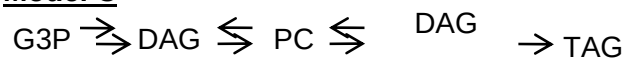


**Model C, variant 1**

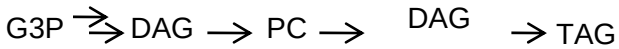


**Model C, variant 2**

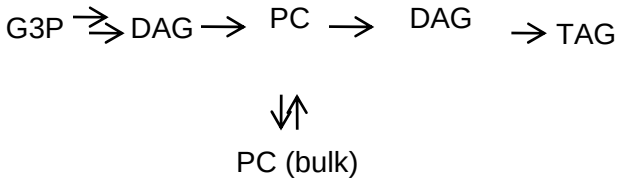


**Model C, variant 3**

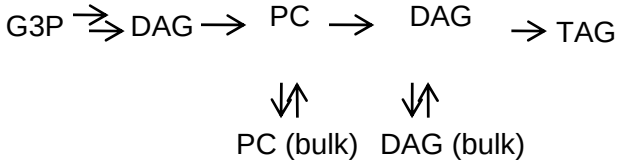


**Figure S8:** Flux models for TAG synthesis which were tested by pool filling simulations of kinetic labeling experiments and which are shown in Figure S9.

**Figure S9:** Pool filling simulations of flux models shown in Figure S8 run to describe the kinetic labeling experiments. Graphs of simulations of acyl pool filling, either from *de novo* DAG acyl labeling (equivalent to glycerol backbone *de novo* labeling), or from acyl editing inputs. The pool filling represents the labeling experiments, where nascent, labeled acyl groups are available from fatty acid synthesis for glycerolipid synthesis.

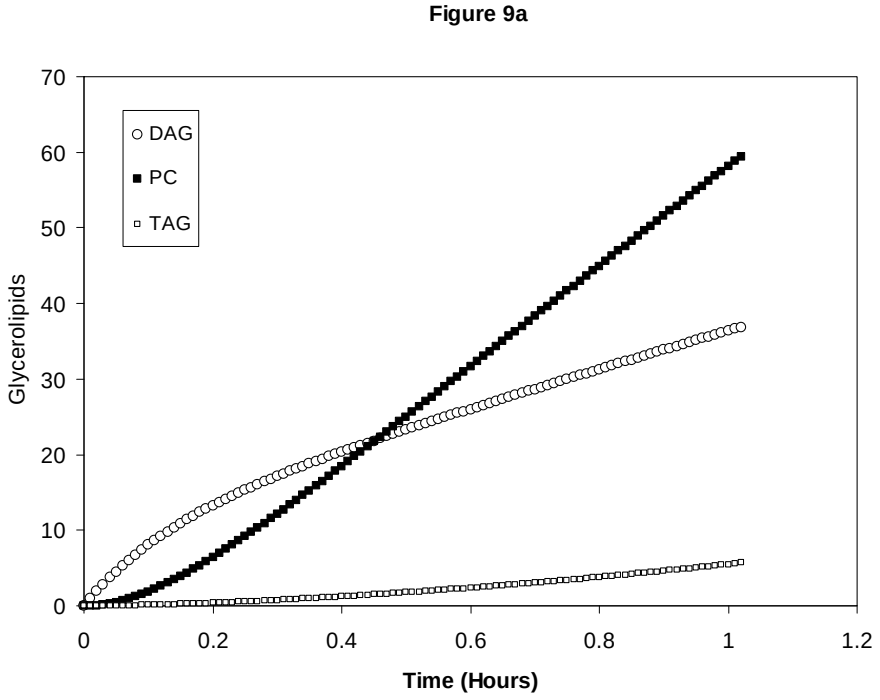


**Figure S9a**: Pool filling from de novo DAG synthesis using model B.

**Figure 9b**

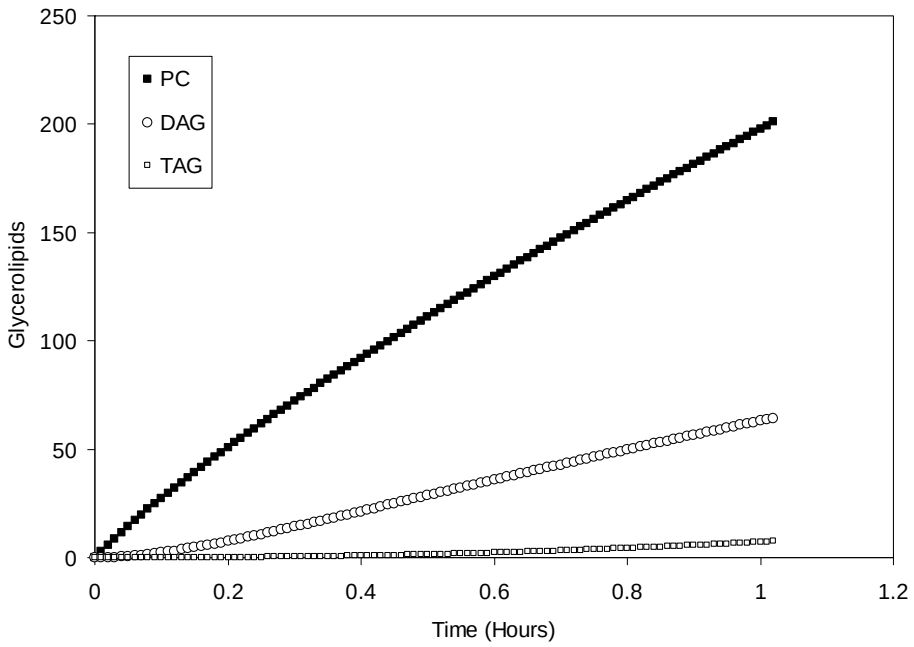


**Figure S9b**: Pool filling from acyl editing using model B.

**Figure 9c**

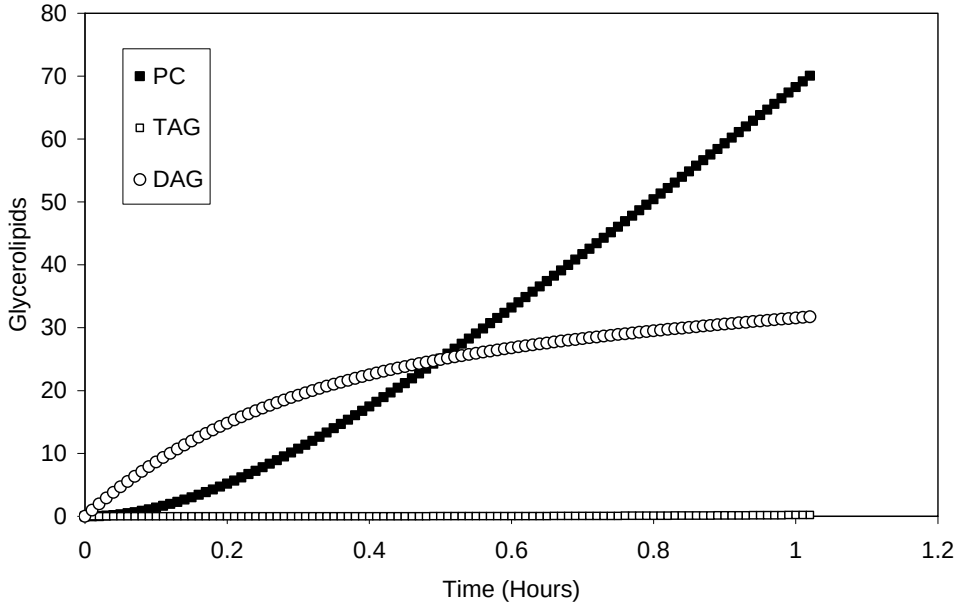


**Figure S9c**: Pool filling from de novo DAG synthesis using model C, variant 1.

**Figure 9d**

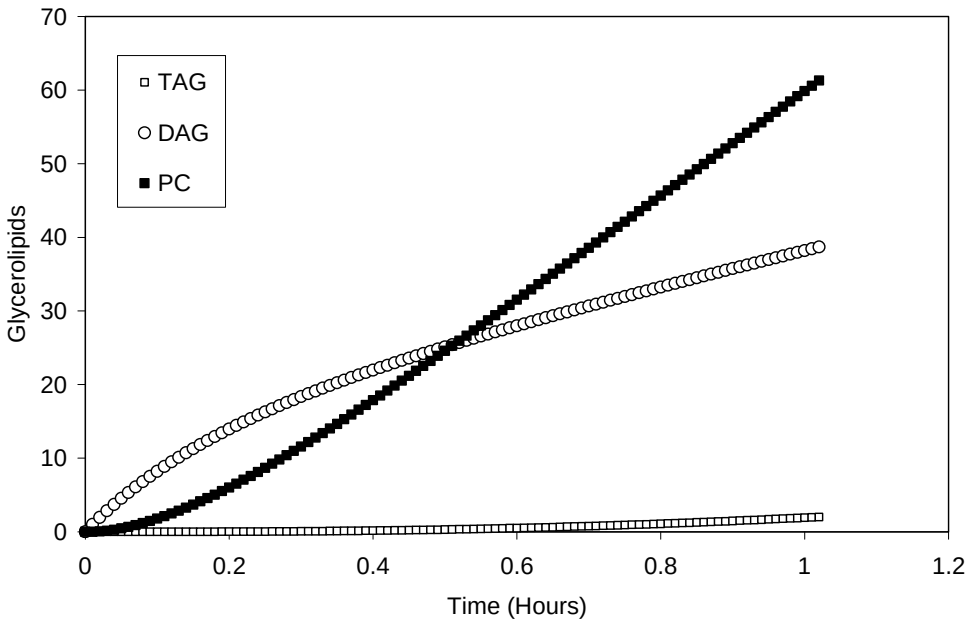


**Figure S9d**: Pool filling from de novo DAG synthesis using model C, variant 2.

**Figure 9e**

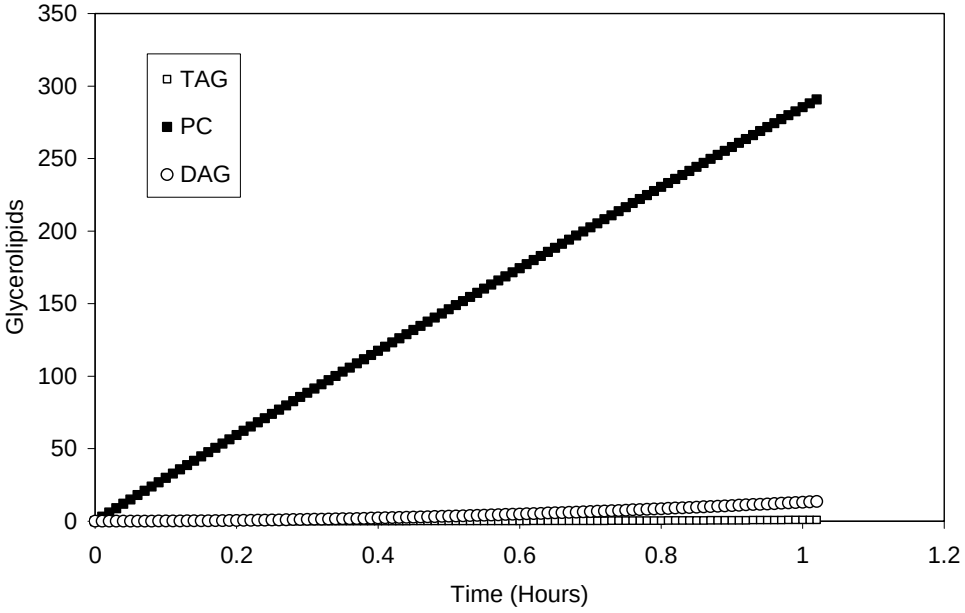


**Figure S9e**: Pool filling from acyl editing via the bulk PC pool using model C, variant 2.

**Figure 9f**

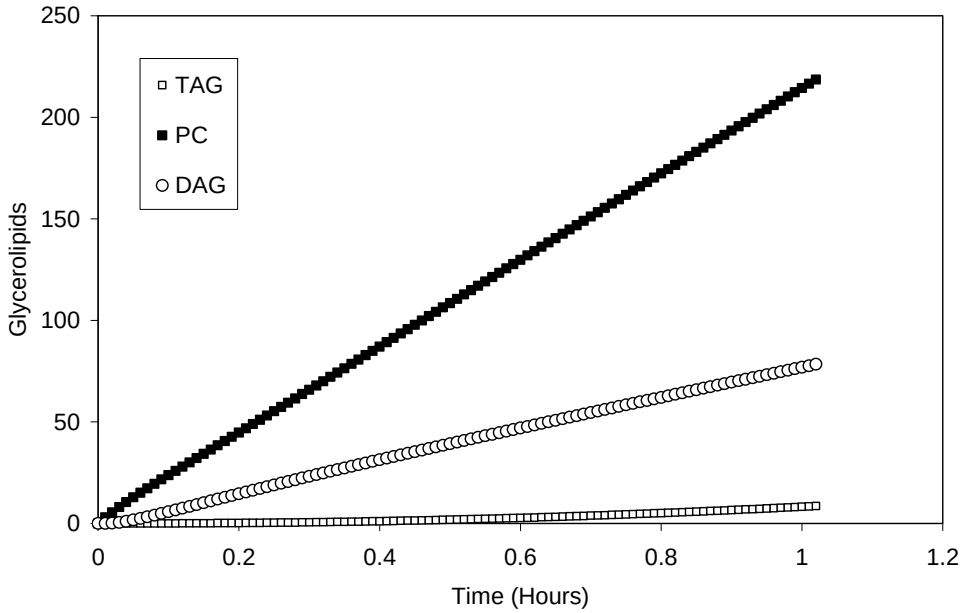


**Figure S9f**: Pool filling from acyl editing via the active PC pool using model C, variant 2.

**Figure 9g**

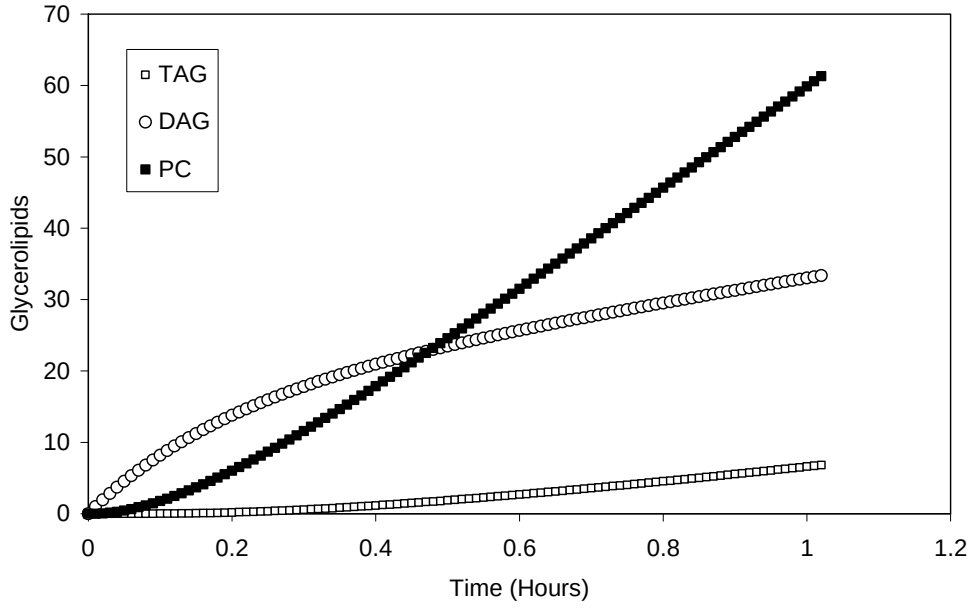


**Figure S9g**: Pool filling from de novo DAG synthesis using model C, variant 3.